CHARACTERISTIC DISSIPATIVE GALERKIN SCHEME FOR OPEN-CHANNEL FLOW

By F. E. Hicks[1] and P. M. Steffler,[2] Associate Members, ASCE

ABSTRACT: Many open-channel flow problems may be modeled as depth-averaged flows. Petrov-Galerkin finite element methods, in which up-wind weighted test functions are used to introduce selective numerical dissipation, have been used successfully for modeling open-channel flow problems. The underlying consistency and generality of the finite element method is attractive because separate computational algorithms for subcritical and supercritical flow are not required and algorithm extension to the two-dimensional depth-averaged flow equations is straightforward. Here, a reconsideration of the fundamental role of the characteristics in the determination of the up-wind weighting and the use of the conservation form of the governing equations, leads to a new Petrov-Galerkin scheme entitled the characteristic dissipative Galerkin method. A linear stability analysis illustrates the selective damping of short wavelengths and excellent phase accuracy achieved by this scheme, as well as its insensitivity to parameter variation. Numerical tests are also presented to illustrate the rugged performance of the scheme. This method could be extended to other hyperbolic systems such as: two-dimensional flows, multilayer fluids, or sediment-transport problems.

INTRODUCTION

Depth-averaged modeling of open-channel flow problems is an increasingly important aspect of hydraulic engineering. Flood-zone delineation and the analysis of surge propagation through compound channels due to dam failures are cases where a depth-averaged flow model could be applied. Advances in computer hardware have made routine calculations of this type practical.

The underlying consistency and generality of the finite element method is attractive for modeling open-channel flow problems. For example, separate computational algorithms for subcritical and supercritical flow are not required. Also, algorithm extension to the two-dimensional depth-averaged flow equations is straightforward, where geometric flexibility and the use of natural boundary conditions are significant advantages.

Katopodes (1984) applied the dissipative Galerkin (DG) scheme to the nonconservation form of the St. Venant equations. In this Petrov-Galerkin finite element method, based on the work of Dendy (1974) and Wahlbin (1974), up-wind weighted test functions are used to introduce numerical dissipation to damp spurious oscillations. The DG scheme has been shown to selectively damp the shortest wavelengths while simultaneously attaining good phase accuracy and has provided very promising results for a number of one-dimensional tests (Katopodes 1984a). It has also been successfully extended to two-dimensional problems (Katopodes 1984a, 1987; Wang and Adeff 1987). Unfortunately, to assure sufficient damping for problems in-

[1]Assoc. Prof., Dept. of Civ. Engrg., Univ. of Alberta, Edmonton, Alberta, Canada, T6G 2G7.

[2]Assoc. Prof., Dept. of Civ. Engrg., Univ. of Alberta, Edmonton, Alberta, Canada.

Note. Discussion open until July 1, 1992. To extend the closing date one month, a written request must be filed with the ASCE Manager of Journals. The manuscript for this paper was submitted for review and possible publication on March 10, 1991. This paper is part of the ***Journal of Hydraulic Engineering***, Vol. 118, No. 2, February, 1992. ©ASCE, ISSN 0733-9429/92/0002-0337/$1.00 + $.15 per page. Paper No. 1540.

volving shocks, the magnitude of the up-winding coefficient in the DG scheme has to be increased (Katopodes 1984).

In this study, a reconsideration of the fundamental role of the characteristics in the determination of the up-wind weighting and the use of the conservation form of the equations leads to a modified approach entitled the characteristic dissipative Galerkin (CDG) scheme, which possesses this shock-handling capability without requiring any parameter variation. The derivation of the CDG scheme is introduced and the characteristics of the up-winding matrix are examined in comparison to the DG scheme. A linear stability analysis is used to compare the phase and amplitude accuracy of the CDG scheme to that of the DG scheme. The CDG scheme is also compared to the commonly used weighted four-point (WFP) implicit finite difference method. Finally, numerical tests are used to verify the performance of the CDG scheme.

One-Dimensional Equations of Open-Channel Flow

Which the method is directed to the solution of two-dimensional flow, the behavior is most easily understood when evaluated through one-dimensional tests. In addition, treatment of the dynamic terms is fundamental. Therefore as an essential first step, the following conservation form of the open-channel flow equations, restricted to one-dimensional, frictionless flow in a horizontal, rectangular channel is considered:

$$\frac{\partial H}{\partial t} + \frac{\partial q}{\partial x} = 0 \quad \ldots\ldots (1)$$

$$\frac{\partial q}{\partial t} + \frac{\partial}{\partial x}\left(\frac{gH^2}{2} + Uq\right) = 0 \quad \ldots\ldots (2)$$

where t = the temporal coordinate; x = the longitudinal coordinate; H = the flow depth; q = the discharge per unit width; U = the cross-sectionally averaged longitudinal velocity; and g = the acceleration due to gravity. Eqs. (1) and (2) may be represented in matrix form as:

$$\frac{\partial \boldsymbol{\phi}}{\partial t} + \frac{\partial \{\mathbf{F}\}}{\partial x} = \mathbf{0} \quad \ldots\ldots (3)$$

where:

$$\boldsymbol{\phi} \equiv \begin{pmatrix} H \\ q \end{pmatrix} \quad \ldots\ldots (4)$$

and,

$$\mathbf{F} \equiv \begin{pmatrix} q \\ Uq + \dfrac{gH^2}{2} \end{pmatrix} \equiv \begin{pmatrix} q \\ Uq + \dfrac{c^2 H}{2} \end{pmatrix} \equiv \begin{bmatrix} 0 & 1 \\ c^2/2 & U \end{bmatrix} \boldsymbol{\phi} \quad \ldots\ldots (5)$$

where $\mathbf{F}$ = the flux vector (dependent upon $\boldsymbol{\phi}$); and c = the celerity.

A nonconservation form of the momentum equation may also be considered:

$$\frac{\partial q}{\partial t} + (gH - U^2)\frac{\partial H}{\partial x} + 2U\frac{\partial q}{\partial x} = 0 \quad \ldots\ldots (6)$$

Eq. (6) can be combined with the continuity equation and presented in matrix form as:

$$\frac{\partial \Phi}{\partial t} + \mathbf{A}\frac{\partial \Phi}{\partial x} = \mathbf{0} \quad \ldots\ldots (7)$$

in which

$$\mathbf{A} \equiv \begin{bmatrix} 0 & 1 \\ (gH - U^2) & 2U \end{bmatrix} \equiv \begin{bmatrix} 0 & 1 \\ (c^2 - U^2) & 2U \end{bmatrix} \quad \ldots\ldots (8)$$

is known as the convection matrix.

As will be demonstrated, integration by parts of the conservation form retains conservation properties and generates appropriate natural boundary conditions. However, construction of the dissipation matrix for the characteristic dissipative-Galerkin scheme is based on the nonconservation form represented by the system in (7).

In the ensuing discussion, matrix notation will continue to be used to indicate the variables and system of equations, while indexes will be used in the nodal discretization.

Finite Element Formulation

The spatial discretization of this system of equations is achieved through the use of linear interpolation (or basis) functions to approximate the behavior of the solution over each element. Therefore,

$$\Phi \approx \tilde{\Phi} = \sum_{j=1}^{M} \mathbf{B}_j \Phi_j \quad \ldots\ldots (9)$$

where

$$\mathbf{B}_j \equiv \begin{bmatrix} b_j & 0 \\ 0 & b_j \end{bmatrix} \quad \ldots\ldots (10)$$

and the trial function $\tilde{\Phi}$ = an approximation to the real solution; and M = the number of nodes in the domain. For the jth node, the basis function used is a standard chapeau function given by:

$$b_j(x) \equiv 0; \qquad x < x_{j-1} \quad \ldots\ldots (11a)$$

$$b_j(x) \equiv \frac{x - x_{j-1}}{x_j - x_{j-1}}; \qquad x_{j-1} < x < x_j \quad \ldots\ldots (11b)$$

$$b_j(x) \equiv \frac{x_{j+1} - x}{x_{j+1} - x_j}; \qquad x_j < x < x_{j+1} \quad \ldots\ldots (11c)$$

$$b_j(x) \equiv 0; \qquad x > x_{j+1} \quad \ldots\ldots (11d)$$

Applying a Petrov-Galerkin weighted residual method to the conservation form of the equations and noting that the integration will actually proceed on an element-by-element basis:

$$\sum_{e=1}^{E} \left\{ \int_{l_e}^{r_e} \left[\mathbf{B}_i \frac{\partial \Phi}{\partial t} - \frac{\partial \mathbf{B}_i}{\partial x}\mathbf{F} + \mathbf{V}_i \left(\frac{\partial \Phi}{\partial t} + \mathbf{A}\frac{\partial \Phi}{\partial x} \right) \right] dx + (\mathbf{B}_i \mathbf{F})\Big|_{l_e}^{r_e} \right\} = \mathbf{0} \quad \ldots\ldots (12)$$

where the flux terms involving the Galerkin component of the test function have been integrated by parts. $\mathbf{V}_i$ represents a 2×2 matrix of the Petrov-Galerkin component of the test functions at the ith node, E is the number of elements, and r_e and l_e represent the right and left boundaries of the eth element, respectively. Examination of last term indicates that if conservation of mass and momentum across internal element boundaries are enforced, only contributions from the domain boundaries (0 and L) remain. These terms represent boundary fluxes of mass and momentum and appear as natural boundary conditions and may therefore be implemented directly.

Substitution of the interpolation functions yields,

$$\int_0^L \left[\mathbf{B}_i \mathbf{B}_j \frac{\partial \mathbf{\Phi}_j}{\partial t} - \frac{\partial}{\partial x} \mathbf{B}_i \begin{bmatrix} 0 & 1 \\ c^2/2 & U \end{bmatrix} \mathbf{B}_j \mathbf{\Phi}_j + \mathbf{V}_i \left(\mathbf{B}_j \frac{\partial \mathbf{\Phi}_j}{\partial t} + \mathbf{A} \frac{\partial \mathbf{B}_j}{\partial x} \mathbf{\Phi}_j \right) \right] dx$$

$$+ \left(\mathbf{B}_i \begin{bmatrix} 0 & 1 \\ c^2/2 & U \end{bmatrix} \mathbf{\Phi}_j \right) \Bigg|_0^L = \mathbf{0} \quad \ldots\ldots (13)$$

This may also be written in matrix notation as:

$$\mathbf{S}_{ij} \left(\frac{\partial \Phi}{\partial t} \right)_j + \mathbf{K}_{ij} \mathbf{\Phi}_j = \mathbf{0} \quad \ldots\ldots (14)$$

where $\mathbf{S}_{ij}$ = the mass matrix; and $\mathbf{K}_{ij}$ = the stiffness matrix (and is dependent upon $\mathbf{\Phi}$).

Eq. (14) represents the semi-discrete form of the problem, which is next discretized in time by using a θ implicit finite difference approximation

$$[(\mathbf{S}_{ij} + \theta \Delta t (\mathbf{K} \tilde{\mathbf{\Phi}}^{n+1})_{ij}] (\mathbf{\Phi}^{n+1})_j = (\mathbf{S}_{ij} - (1 - \theta) \Delta t (\mathbf{K} \tilde{\mathbf{\Phi}}^n)_{ij}] (\mathbf{\Phi}^n)_j \quad \ldots\ldots (15)$$

A Newton-Raphson interation was employed to solve this nonlinear system. Convergence was assessed based on a norm of the vector of corrections compared to a specified tolerance, specifically if

$$\frac{\Sigma[(\delta \mathbf{\Phi})^2]}{\Sigma(\mathbf{\Phi}^2)} \leq \text{tolerance} \quad \ldots\ldots (16)$$

then the solution would progress to the next time step.

Choice of Test Functions

The dissipative schemes considered in this study employ the following form of the test function

$$\mathbf{V}_i \equiv \omega \mathbf{W} \frac{\Delta x}{2} \frac{d}{dx} \mathbf{B}_i \quad \ldots\ldots (17)$$

in which, ω = a dissipation parameter (or up-winding coefficient) dependent upon the flow situation. $\mathbf{W}$ represents an up-winding matrix that controls the distribution of the numerical dissipation. The components of the up-winding matrix:

$$\mathbf{W} \equiv \begin{bmatrix} w_{aa} & w_{aq} \\ w_{qa} & w_{qq} \end{bmatrix} \quad \ldots\ldots (18)$$

control the weighted combinations of the contributions of the continuity and momentum equations to the up-winding. The first letter in the component subscript denotes the equation in which the up-winding contribution applies (a for continuity and q for momentum), while the second describes the equation on which it operates. For example, w_{aq} represents the coefficient applied to the momentum equation contribution in up-winding the continuity equation.

Evaluating the integrals element by element, the resulting element matrices become:

$$\mathbf{S}_e \equiv \begin{bmatrix} \int_e \left[(b_i b_j) + \left(w_{aa}\omega \frac{\Delta x}{2} \frac{db_i}{dx} b_j \right) \right] dx & \int_e \left(w_{aq}\omega \frac{\Delta x}{2} \frac{db_i}{dx} b_j \right) dx \\ \int_e \left(w_{qa}\omega \frac{\Delta x}{2} \frac{db_i}{dx} b_j \right) dx & \int_e \left[(b_i b_j) + \left(w_{qq}\omega \frac{\Delta x}{2} \frac{db_i}{dx} b_j \right) \right] dx \end{bmatrix} \quad \ldots (19)$$

$$\mathbf{K}_e \equiv \begin{bmatrix} k_{aa} & k_{aq} \\ k_{qa} & k_{qq} \end{bmatrix} \quad \ldots (20)$$

where

$$k_{aa} \equiv \int_e \omega \frac{\Delta x}{2} w_{aq}(gH - U^2) \left(\frac{db_i}{dx} \frac{db_j}{dx} \right) dx \quad \ldots (21)$$

$$k_{qa} \equiv \int_e \left[\left(- \frac{gH}{2} \frac{db_i}{dx} b_j \right) + \omega \frac{\Delta x}{2} w_{qq}(gH - U^2) \left(\frac{db_i}{dx} \frac{db_j}{dx} \right) \right] dx \quad \ldots (22)$$

$$k_{aq} \equiv \int_e \left\{ - \frac{db_i}{dx} b_j + \omega \frac{\Delta x}{2} \left[w_{aa} \frac{db_i}{dx} \frac{db_j}{dx} + w_{aq}(2U) \frac{db_i}{dx} \frac{db_j}{dx} \right] \right\} dx \quad \ldots (23)$$

$$k_{qq} \equiv \int_e \left[\left(-U \frac{db_i}{dx} b_j \right) + \omega \frac{\Delta x}{2} \left\{ [w_{qa} + w_{qq}(2U) \frac{db_i}{dx} \frac{db_j}{dx} \right\} \right] dx \quad \ldots (24)$$

Specification of Up-Winding Matrix

The DG method (Katopodes 1984) is defined by the following choice of up-winding matrix (for $U > 0$):

$$\mathbf{W} \equiv \frac{\mathbf{A}}{|U + c|} = \begin{bmatrix} 0 & 1/|U + c| \\ (c^2 - U^2)/|U + c| & 2U/|U + c| \end{bmatrix} \quad \ldots (25)$$

The CDG method is based upon the work of Hughes and Mallet (1986) who examined the application of Petrov-Galerkin methods to symmetric systems of hyperbolic equations. In general, implementation requires that

$$\mathbf{W} = \frac{\mathbf{A}}{|\mathbf{A}|} \quad \ldots (26)$$

Decomposing **A**

$$\mathbf{A} = \mathbf{M}\Lambda\mathbf{M}^{-1} = \begin{bmatrix} 1/2c & -1/2c \\ (U + c)/2c & -(U - c)/2c \end{bmatrix}$$

$$\begin{bmatrix} U + c & 0 \\ 0 & U - c \end{bmatrix} \begin{bmatrix} -(U - c) & 1 \\ -(U + c) & 1 \end{bmatrix} \quad \ldots\ldots\ldots\ldots\ldots\ldots\ldots\ldots\ldots\ldots (27)$$

in which

$$\Lambda \equiv \begin{bmatrix} \lambda_1 & 0 \\ 0 & \lambda_2 \end{bmatrix} \text{ where } \quad \lambda_i = U \pm c \text{ for } i = 1, 2 \quad \ldots\ldots\ldots\ldots\ldots (28)$$

are the characteristic velocities, (26) can be evaluated as:

$$\mathbf{W} = \mathbf{M} \begin{bmatrix} \lambda_1/|\lambda_1| & 0 \\ 0 & \lambda_2/|\lambda_2| \end{bmatrix} \mathbf{M}^{-1} = \begin{bmatrix} 1/2c & -1/2c \\ (U + c)/2c & -(U - c)/2c \end{bmatrix}$$

$$\begin{bmatrix} (U + c)/|U + c| & 0 \\ 0 & (U - c)/|U - c| \end{bmatrix} \begin{bmatrix} -(U - c) & 1 \\ -(U + c) & 1 \end{bmatrix} \quad \ldots\ldots\ldots\ldots (29)$$

It may be noted that each characteristic velocity is used in the determination of the up-winding matrix. Therefore, this method is introduced here as the characteristic dissipative Galerkin (CDG) method for modeling open-channel flow.

In contrast, it can be shown that the up-winding matrix for the DG scheme is equivalent to:

$$\mathbf{W} = \boldsymbol{M} \begin{bmatrix} \lambda_1/|\lambda_1| & 0 \\ 0 & \lambda_2/|\lambda_1| \end{bmatrix} \mathbf{M}^{-1} = \begin{bmatrix} 1/2c & -1/2c \\ (U + c)/2c & -(U - c)/2c \end{bmatrix}$$

$$\begin{bmatrix} (U + c)/|U + c| & 0 \\ 0 & (U - c)/|U + c| \end{bmatrix} \begin{bmatrix} -(U - c) & 1 \\ -(U + c) & 1 \end{bmatrix} \quad \ldots\ldots\ldots\ldots (30)$$

Thus, it is seen that the up-winding matrix for the DG scheme is scaled using the positive characteristic, $\lambda_1 = (U + c)$, only. Clearly, the magnitude of the up-winding applied to the regressive wave may be too small.

The two schemes may be further compared by writing the up-winding matrices in terms of the local Froude number

$$\mathsf{F} = \frac{U}{c} \quad \ldots\ldots\ldots\ldots\ldots\ldots\ldots\ldots\ldots\ldots\ldots\ldots\ldots\ldots\ldots\ldots\ldots\ldots (31)$$

For the DG scheme, the upwinding matrix becomes:

$$\mathbf{W} \equiv \begin{bmatrix} 0 & 1/c\ 1/|\mathsf{F} + 1| \\ c[-(\mathsf{F} + 1)(\mathsf{F} - 1)]/|\mathsf{F} + 1| & 2\mathsf{F}/|\mathsf{F} + 1| \end{bmatrix} \quad \ldots\ldots\ldots\ldots (32a)$$

while for the CDG scheme

$$\mathbf{w} \equiv \begin{bmatrix} (1 - \mathsf{F}^2)/2\ (1/|\mathsf{F} + 1| - 1/|\mathsf{F} - 1|) & 1/2c((\mathsf{F} + 1)/|\mathsf{F} + 1| - (\mathsf{F} - 1)/|\mathsf{F} - 1|) \\ c/2(1 - \mathsf{F}^2)((\mathsf{F} + 1)|\mathsf{F} + 1/| - (\mathsf{F} - 1)/|\mathsf{F} - 1|) & 1/2((\mathsf{F} + 1)^2/|\mathsf{F} + 1| - (\mathsf{F} - 1)^2/|\mathsf{F} - 1|) \end{bmatrix} \quad \ldots\ldots (33)$$

Fig. 1 illustrates the up-winding matrices for these two schemes, for $\mathsf{F} > 0$. They are identical at $\mathsf{F} = 0$ where:

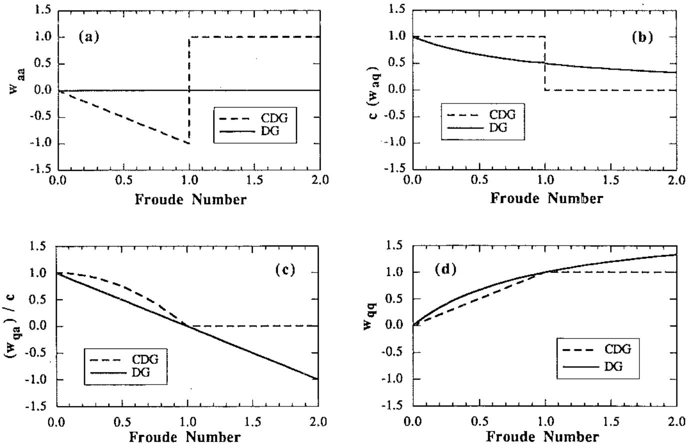

FIG. 1. Variation of Up-Winding Matrix with Froude Number

$$\mathbf{W}_{\mathsf{F}=0} = \begin{bmatrix} 0 & 1/c \\ c & 0 \end{bmatrix} \quad (34)$$

that is, up-winding contributions to the continuity equation come only from the momentum equation, while up-winding contributions to the momentum equation come only from the continuity equation.

At $\mathsf{F} = 1$ they intersect where

$$\mathbf{W}_{\mathsf{F}=1} = \begin{bmatrix} 0 & 1/2c \\ c & 1 \end{bmatrix} \quad (35)$$

For subcritical flow, only the momentum equation is used in up-winding continuity equation in the DG scheme, with the magnitude of the up-winding term decreasing with increasing Froude number. The CDG achieves a similar effect by reducing the constant up-winding contribution from the momentum equation with a linearly decreasing negative up-winding contribution from the continuity equation. Up-winding contributions in the momentum equation are handled quite similarly for the two methods. The up-winding contribution from the continuity equation decreases with increasing Froude number, while the contribution from the momentum equation decreases.

For supercritical flow, again, the up-winding of the continuity equation in the DG scheme comes only from the momentum equation, and decreases with increasing Froude number. For the momentum equation, the DG scheme counteracts an increasing contribution from the momentum equation with a linearly decreasing negative up-winding contribution from the continuity equation. From the figure, it appears that both w_{qa} and w_{qq} continue to increase in magnitude with increasing Froude number beyond $\mathsf{F} = 2$. For supercritical flow, the up-winding matrix for the CDG scheme is constant and equal to:

$$\mathbf{W}_{\mathrm{CDGF}>1} = \begin{bmatrix} 1 & 0 \\ 0 & 1 \end{bmatrix} \quad (36)$$

Linear Stability Analysis

Katopodes (1984b) and Froehlich (1985) have examined the amplification and phase characteristics of the DG scheme for the linearized St. Venant equations by Fourier analysis. Although such an analysis cannot predict instabilities associated with nonlinearities in the problem, it is a valuable tool as a basis for the comparison of various numerical schemes and also helps to determine the appropriate discretization of a problem for a particular method.

The nondimensional linearized form of the St. Venant equations used in the linear stability analysis of the CDG scheme may be written:

$$\frac{\partial \boldsymbol{\phi}_*}{\partial t_*} + \begin{bmatrix} 0 & 1 \\ 1 - \mathsf{F}_o^2 & 2\mathsf{F}_o \end{bmatrix} \frac{\partial \boldsymbol{\phi}_*}{\partial x_*} = \mathbf{0} \quad \ldots\ldots (33)$$

where $\boldsymbol{\phi}_*$, t_*, and x_* are defined by:

$$x_* = \frac{x}{L}; \qquad t_* = \frac{tL}{U}; \qquad \boldsymbol{\phi}_* = \begin{bmatrix} H/H_o \\ q/(U_o H_o) \end{bmatrix} \quad \ldots\ldots (38)$$

where L = a length scale; H_o and U_o = the uniform flow depth and velocity, respectively; and F_o is the Froude number of the uniform flow, defined by

$$\mathsf{F}_o \equiv \frac{U_o}{\sqrt{gH_o}} \quad \ldots\ldots (39)$$

Each Fourier component of the solution may assume the form (Roache 1982):

$$(\boldsymbol{\phi}_*)^{n+1}(x_*) = \boldsymbol{\Phi}^{n+1} \exp(ikx_*) \quad \ldots\ldots (40)$$

where $\boldsymbol{\Phi}^{n+1}$ = the solution amplitude at time $n + 1$

$$i \equiv \sqrt{-1} \quad \ldots\ldots (41)$$

and k = the component wave number, such that

$$k \equiv \frac{2\pi}{\lambda} \quad \ldots\ldots (42)$$

where λ = the wavelength. The number of discretizations per wavelength, N, is then

$$N \equiv \frac{\lambda}{\Delta x} \quad \ldots\ldots (43)$$

The complex amplification matrix, $\mathbf{G}$, defined such that

$$\boldsymbol{\Phi}^{n+1} = \mathbf{G}\boldsymbol{\Phi}^n \quad \ldots\ldots (44)$$

describes both the amplification and phase characteristics of the numerical method. The two complex eigenvalues of this matrix, corresponding to the regressive and progressive waves, can be written in the form:

$$re^{i\Theta} \quad \ldots\ldots (45)$$

where r = the magnification factor or the algorithmic damping coefficient; and Θ = the numerical phase shift, that is:

$$\Theta \equiv k\Delta x_* \quad \ldots\ldots (46)$$

where Δx_* = the distance moved by the wave. The relative celerity of the progressive and regressive waves are defined by:

$$\text{relative celerity} \equiv \frac{\Theta}{\Theta_{\text{anal}}} = \frac{\Theta}{\mp \frac{2\pi}{N} \frac{(U \pm c)\,\Delta t_*}{\Delta x_*}} \quad \ldots\ldots (47)$$

The value of the up-winding coefficient, ω, has been the subject of some investigation. Brooks and Hughes (1982) report that for the steady one-dimensional convection diffusion equation, a value of $\omega = 1.0$ is optimum in that it leads to exact solutions at the nodes in the limit as diffusion goes to zero. For the transient case, an optimum can be based on minimizing phase error. For the one-dimensional convection equation, Raymond and Garder (1976) showed that a value of $\omega = 2/\sqrt{15}$ ($\omega \approx 0.50$) would minimize phase error (Brooks and Hughes 1982). Katopodes (1984) examined several values of ω for the DG scheme applied to the open-channel flow equations, including $\omega = 2/\sqrt{15}$ and $\omega = \Delta t|U + c|/\Delta x$. In order to ensure stability, larger values of ω were required to overcome inadequate damping of regressive waves when modeling shocks. He concluded that numerical experimentation would be required to quantify an optimum value. Froehlich (1985) illustrated the effect of varying the up-winding coefficient on the phase and amplitude accuracy of this scheme for the linear equations and demonstrated a great sensitivity to Courant number at the shorter wavelengths. The Courant number, C, is defined as

$$C = \frac{(U + c)\Delta t}{\Delta x} \quad \ldots\ldots (48)$$

To examine the sensitivity of the CDG scheme to this up-winding coefficient, Fourier analysis was performed at three values of ω: 0.25, 0.5, and 1.0. It was determined that a value of $\omega = 0.5$ provides both good phase accuracy and highly selective damping (Hicks and Steffler 1990). Therefore, $\omega = 0.5$ was accepted as appropriate for the CDG scheme.

Fig. 2 illustrates the results of the linear stability analysis for progressive waves at any Froude number, for Courant numbers of 0.5 and 1.0. The CDG scheme is particularly successful at damping the shortest wavelengths and a Courant number of 0.5 is indicated as appropriate in order to balance time and space errors. In fact, the CDG scheme works well over a range of values up to $C = 0.5$. For comparison purposes, results for the WFP scheme, run at $\theta = 0.6$ [as recommended by Fread (1988)], are shown as well. At a Courant number of 0.5 the WFP scheme displays less selective damping charactgeristics with less damping of short waves and more damping of long waves. Phase accuracy is also worse. When the Courant number is increased to 1, excellent phase accuracy is achieved, but at the expense of introducing excessive algorithmic damping.

For regressive waves, both the CDG and the WFP schemes display selective damping of the shortest wavelengths. However, as seen in Fig. 3 for $F = 0.5$ and 2.0, the WFP method exhibits poor phase accuracy at both C

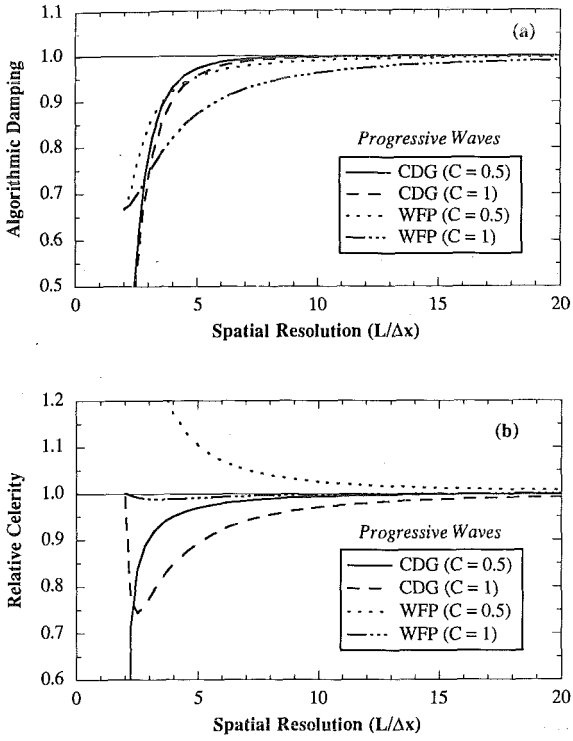

FIG. 2. Results of Linear Stability Analysis for Progressive Waves for CDG (ω = 0.5, θ = 0.5) and WFP (θ = 0.6) Schemes. (*a*) Algorithmic Damping; (*b*) Relative Celerity

= 0.5 and $C = 1$. Again, as in the case of the progressive waves, the CDG displayed excellent phase accuracy at $C = 0.5$.

Figs. 4 and 5 compare the amplitude and phase accuracy of the DG and CDG methods at short wavelengths, for $\omega = 0.5$, $C = 0.5$, $F = 0.5$, and $\theta = 0.5$. Also included in the plots are results for the DG scheme for a value of the up-winding coefficient increased by a factor of 7.5 (corresponding to $\omega = \Delta t|U + c|/\Delta x$ used by Katopodes (1984a) in modeling a stationary hydraulic jump). As seen in Fig. 4, with $\omega = 0.5$, the performance of the DG and CDG schemes for progressive waves is virtually identical. Increasing the value of ω for the DG scheme does not increase the damping on the very short wavelengths (less than 4 or 5) but does significantly affect the phase accuracy. The difference between the DG and CDG schemes becomes clear when considering the regressive waves. As Fig. 5 shows, for $\omega = 0.5$, the CDG is more dissipative than the DG for short wavelengths and it also displays better phase accuracy. When ω is increased for the DG method, the regressive wave damping is increased while the phase accuracy is substantially reduced.

NUMERICAL TESTS

As the linear stability analysis indicates, the advantage of the refinement from the DG to the CDG scheme lies in the consideration of both char-

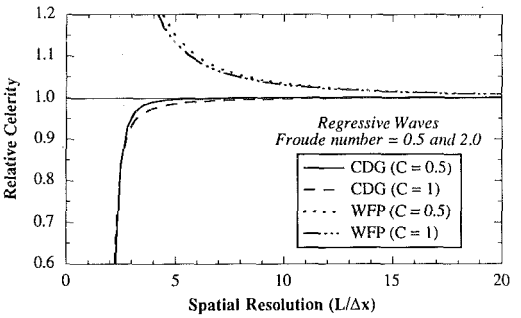

FIG. 3. Relative Celerity of CDG ($\omega = 0.5$, $\theta = 0.5$) and WFP ($\theta = 0.6$) Schemes for Regressive Waves, F = 0.5 and 2.0

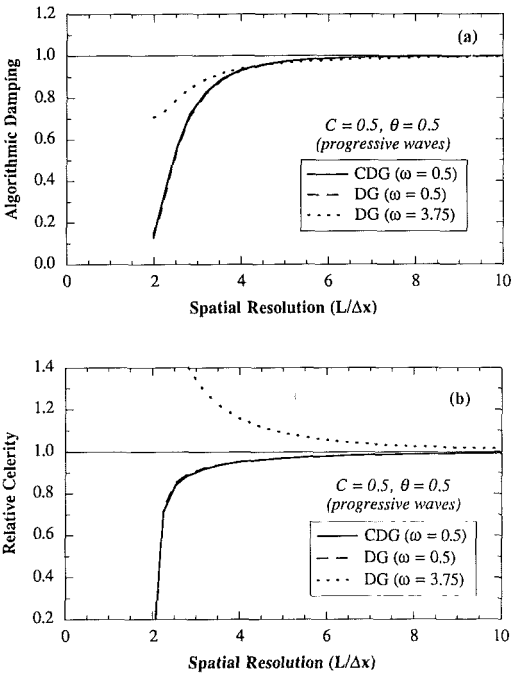

FIG. 4. Comparison of Results of Linear Stability Analysis for Progressive Waves for DG and CDG Schemes for $C = 5$, $\theta = 0.5$. (*a*) Algorithmic Damping; (*b*) Relative Celerity

acteristics in quantifying the up-winding. This leads to the enhanced ability of the CDG scheme to handle shocks without requiring an increase in the up-winding coefficient ω. To illustrate this, a numerical test involving the transition from a supercritical to a subcritical flow in a horizontal, frictionless channel was adapted from a steady flow test of Katopodes (1984a). The test was designed to combine a disturbance propagation problem with a steady

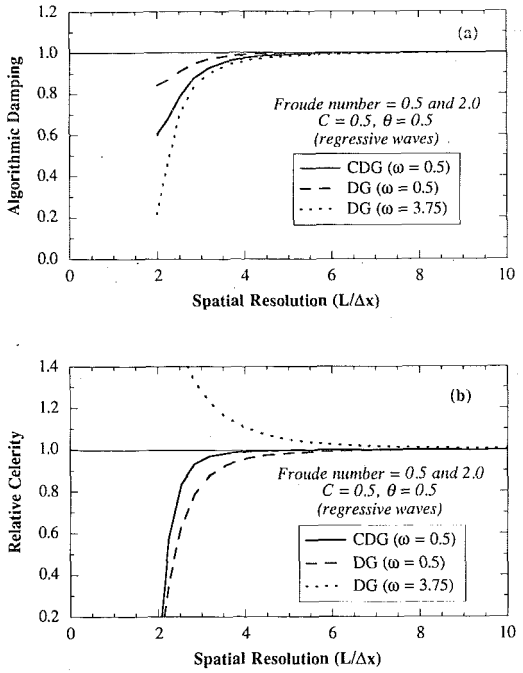

FIG. 5. Comparison of Results of LinearStability Analysis for Regressive Waves for DG and CDG Schemes for $C = 5$, $\theta = 0.5$, for F = 0.5 and 2.0. (*a*) Algorithmic Damping; (*b*) Relative Celerity

hydraulic jump situation. Practically speaking, this might occur when routing a flood wave through a long channel involving both mild and steep reaches.

The initial conditions for the unsteady flow test are illustrated in Fig. 6. Sixty nodes, spaced at 5-m intervals, were used in the analysis with the hydraulic jump located 100 m from the upstream end of the channel. The supercritical and subcritical flow depths were set to 1.008 m and 1.80 m, respectively. The corresponding discharge was 5 m^3/s, representing Froude numbers of 1.58 and 0.66, respectively. A triangular disturbance 1.0 m high spread over 10 elements was superimposed just upstream of the jump. The initial discharge was calculated based on the criterion that the wave would be translated entirely to the right. The boundary conditions provided were depth and discharge at the upstream end, and depth at the downstream end. The results are also presented in Fig. 6, after 120 time steps using $\theta = 0.5$ and Δt of 0.2086 s, corresponding to a Courant number of 0.5.

As the figure shows, the CDG method (run at $\omega = 0.5$) preserved the jump well with only minor localized oscillations. However, the DG scheme run at $\omega = 0.5$ was subject to oscillations in the vicinity of the jump. To examine the DG method as it was run by Katopodes (1984), the up-winding coefficient was increased by a factor of $|U + c|$. Although this was successful in suppressing these oscillations and preserving the jump face, the peak flow depth of the propagated wave was reduced by about 15%. In addition, large oscillations, due to phase lead error (predicted by the Fourier analysis in Fig. 4), were observed ahead of this wave.

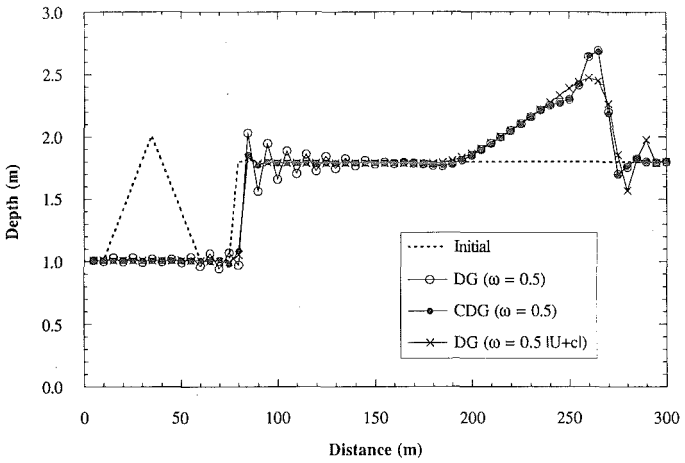

FIG. 6. Propagation of Wave through Hydraulic Jump with Upstream Froude Number of 1.58

Because the inflow and outflow at the domain boundaries remained steady at 5 m^3/s throughout the simulation and the boundary depths remained constant, both mass and total momentum contained in the domain should have remained constant. A comparison between initial and final conditions confirmed the mass and momentum were conserved to at least six significant figures. That is, the CDG scheme up-winding was found to have no effect on the conservation properties of the equations modeled.

To examine the range of applicability of this numerical scheme, this test was repeated using a downstream depth of 6.291 m and a discharge of 15 cms, representing upstream and downstream Froude numbers of 4.79 and 0.31, respectively. This situation is more typical of that encountered in a hydraulic structure rather than in a natural channel. The same disturbance, 1.0 m high spread over 10 elements was superimposed just upstream of the jump, and again the initial discharge was calculated based on the criterion that the wave would be translated entirely to the right. The results are presented in Fig. 7, after 120 time steps using $\theta = 0.5$ and Δt of 0.1135 s, corresponding to a Courant number of 0.5. An additional test with upstream and downstream Froude numbers of 9.58 and 0.20, respectively, failed to converge for either the DG or CDG schemes.

CONCLUSIONS

This study introduces a new Petrov-Galerkin finite element method for solving open-channel flow problems, entitled the characteristic dissipative Galerkin scheme. Results of a linear stability analysis show this scheme to be particularly successful at damping the shortest wavelengths while achieving excellent phase accuracy for Courant number of 0.5 and less. At comparable Courant numbers, the weighted four-point implicit finite difference scheme (used in the familiar DAMBRK code) scheme displays less selective damping and poorer phase accuracy. The weighted four-point scheme achieves excellent phase accuracy when the Courant number is increased to 1, but at the expense of introducing excessive algorithmic damping.

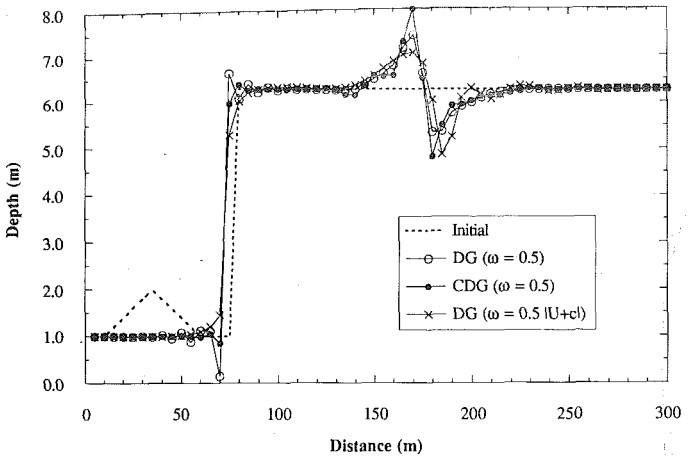

FIG. 7. Propagation of Wave through Hydraulic Jump with Upstream Froude Number of 4.79

The deviation of the characteristic dissipative Galerkin scheme reveals the fundamental role of the characteristics in the determination of the up-wind weighting. The consideration of both characteristics amounts to a refinement of the dissipative Galerkin method, which leads to the ability of the characteristic dissipative Galerkin scheme to handle shocks without requiring an increase in the up-winding coefficient. In contrast, to assure sufficient damping for problems involving shocks, the magnitude of the up-winding coefficient in the dissipative Galerkin method has to be increased. This magnification of the up-winding coefficient leads to less selective damping and a deterioration in phase accuracy.

The refinement required to convert to the characteristic dissipative Galerkin scheme requires no additional computational expense and is relatively simple to implement. Furthermore, use of the conservation form of the St. Venant equations has been shown to conserve both mass and momentum. The CDG method may be extended with confidence to other hyperbolic systems such as two-dimensions depth-averaged flow, multilayer fluids or sediment-transport problems.

ACKNOWLEDGMENTS

This research was financially supported through scholarships to the first writer from: the Natural Sciences and Engineering Research Council of Canada, the Alberta Heritage Scholarship Foundation, the University of Alberta (Faculty of Graduate Studies), the North American Life Assurance Co. with the Canadian Council of Professional Engineers, and the Province of Alberta. All are most gratefully acknowledged. The writers would also like to thank N. Katopodes, R. Gerard, and N. Rajaratnam for their advice during the course of this study.

APPENDIX I. REFERENCES

Brooks, A. N., and Hughes, T. J. R. (1982). "Streamline upwind/Petrov-Galerkin formulations for convection dominated flows with particular emphasis on the in-

compressible Navier-Stokes equations." *Comput. Methods Appl. Mech. Engrg.*, 32, 199–259.
Dendy, J. E. (1974). "Two methods of Galerkin-type achieving optimum L^2 rates of convergence for first-order hyperbolics." *SIAM J. Numer. Anal.*, 11(3), 637–653.
Fread, D. L. (1988). *The NWS DAMBRK model: Theoretical background/user documentation.* Nat. Weather Service (NWS), Silver Spring, Md.
Froehlich, D. C. (1985). Discussion of "A dissipative Galerkin scheme for open-channel flow," by N. D. Katopodes. *J. Hydr. Engrg.*, ASCE, 111(4), 1200–1204.
Hicks, F. E., and Steffler, P. M. (1990). "Finite element modeling of open channel flow." *Water Resour. Engrg. Report No. 90-6,* Univ. of Alberta, Alberta, Canada.
Hughes, T. J. R., and Mallet, M. (1986). "A new finite element formulation for computational fluid dynamics: III. The generalized streamline operator for multidimensional advective-diffusive systems." *Comput. Methods Appl. Mech. Engrg.*, 58(3), 305–328.
Katopodes, N. D. (1984a). "A dissipative Galerkin scheme for open-channel flow." *J. Hydr. Engrg.*, 110(4), 450–466.
Katopodes, N. D. (1984b). "Fourier analysis of dissipative FEM channel flow model." *J. Hydr. Engrg.*, 110(7), 927–944.
Katopodes, N. D. (1987). "Analysis of transient flow through broken levees." *Turbulence measurements and flow modeling,* C. J. Chen, L. D. Chen, and F. M. Holly, Jr., eds., Hemisphere Publishing Corp., Washington, D.C., 301–310.
Raymond, W. H., and Garder, A. (1976). "Selective damping in a Galerkin method for solving wave problems with variable grids." *Monthly Weather Review,* 104(12), 1583–1590.
Roache, P. J. (1982). *Computational fluid dynamics.* Hermosa Publishers, Albuquerque, N.M.
Wang, S. S., and Adeff, S. E. (1987). "A depth integrated model for solving Navier-Stokes equations using dissipative Galerkin scheme." *Turbulence measurements and flow modeling,* C. J. Chen, L. D. Chen, and F. M. Holly, Jr., eds. Hemisphere Publishing Corp., Washington, D.C., 311–321.
Wahlbin, L. B. (1974). "A dissipative Galerkin method for the numerical solution of first order hyperbolic equations." *Mathematical aspects of finite elements in partial differential equations,* C. de Boor, ed., Academic Press, New York, N.Y.

APPENDIX II. NOTATION

The following symbols are used in this paper:

$\mathbf{A}$ = convection matrix;
$\mathbf{B}$ = matrix of interpolation (trial) functions used in finite element method;
c = celerity;
C = Courant number;
F = flux vector;
F = local Froude number;
F_o = uniform flow Froude number;
g = acceleration due to gravity;
G = amplification factor in stability analysis;
H = flow depth;
H_o = uniform flow depth;
i,j,n = integer indices;
k = wave number;
$\mathbf{K}$ = stiffness matrix;
L = length of domain;
M = number of nodes in domain;
N = number of nodes per wavelength;

q = discharge per unit width of channel;
r = algorithmic damping;
$\mathbf{S}$ = mass matrix
t = time coordinate;
t_* = nondimensional time coordinate;
U = cross-sectionally averaged longitudinal velocity;
U_o = uniform flow velocity;
$\mathbf{V}$ = matrix of test functions used in finite element method;
x = longitudinal coordinate;
x_* = nondimensional longitudinal coordinate;
$\mathbf{W}$ = up-winding matrix;
Θ = phase shift angle;
θ = implicitness;
$\mathbf{\Lambda}$ = eigenvalue matrix;
λ = wavelength;
λ_i = characteristic velocities;
Φ = nodal values of solution;
$\boldsymbol{\phi}$ = solution vector;
$\boldsymbol{\phi}_*$ = nondimensional solution vector; and
ω = up-winding coefficient.